Exploring the Mycobacterium tuberculosis antigenome: New insights for the development of vaccines, diagnostics and drugs
Coppola, M.

Citation
Coppola, M. (2022, November 3). *Exploring the Mycobacterium tuberculosis antigenome: New insights for the development of vaccines, diagnostics and drugs*. Retrieved from https://hdl.handle.net/1887/3485193

CHAPTER 4

Mycobacterium tuberculosis in vivo expressed antigens recognized in three genetically different mouse models after *Mycobacterium tuberculosis* infection and BCG vaccination.

Mariateresa Coppola[1]*, Fabienne Jurion[2], Susan J. F. van den Eeden[1], Hermann Giresse Tima[2], Kees L. M. C. Franken[1], Annemieke Geluk[1], Marta Romano[2#] and Tom H. M. Ottenhoff[1#]
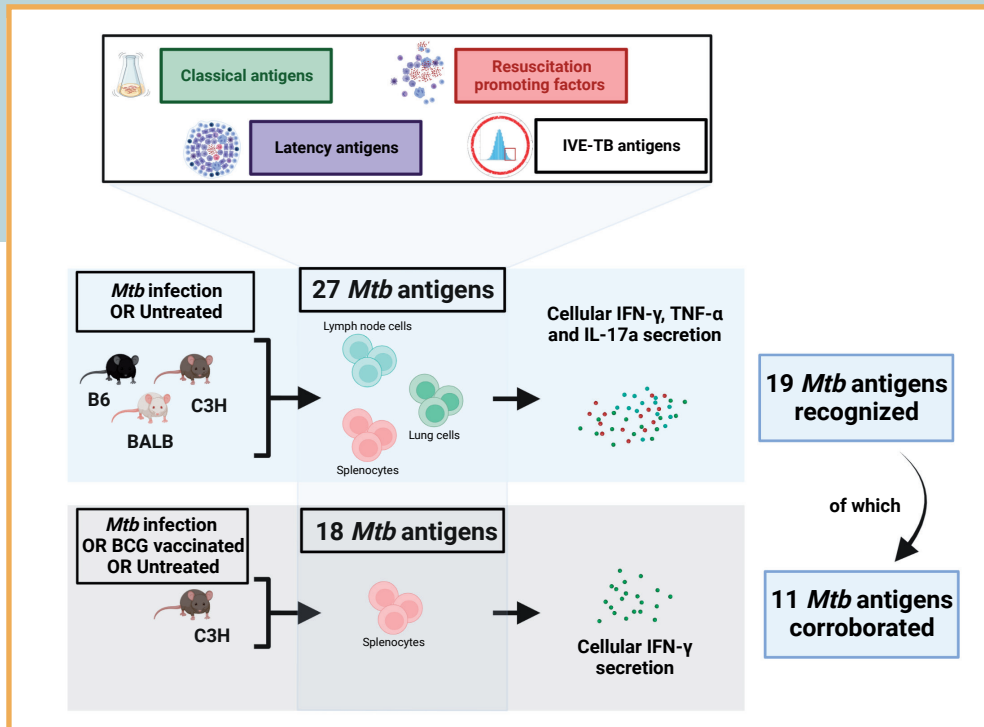
[1]: Department of Infectious Diseases, Leiden University Medical Center, Leiden, The Netherlands
[2]: *In vivo* models unit, Immune Response Service; Infectious Diseases in Humans Scientific Directorate, Sciensano, Belgium
[#]:These authors contributed equally to this work

ABSTRACT

For centuries, tuberculosis (TB) has been a threat to human health. Sadly, TB remains the leading cause of death caused by a single bacterial pathogen and its causative agent, *Mycobacterium tuberculosis* (*Mtb*), has become a major contributor to the emerging antimicrobial resistance global crisis. A major challenge to TB control is the lack of a more effective vaccine than the widely used Bacillus Calmette-Guérin (BCG), which only partially protects against TB. Several new TB vaccine candidates have advanced through the clinical TB vaccine pipeline. However, only M72/AS01E thus far demonstrated significant vaccine efficacy (50%) in preventing progression towards active TB among latently *Mtb* infected individuals. While these results are encouraging there remains a clear need for developing further improved vaccines, likely including additional *Mtb* antigens to broaden the vaccine mobilized immune repertoire.

Novel TB vaccines preferably should be able to (I) boost host immune responses induced by previous infant BCG vaccination and (II) be directed against *Mtb* proteins expressed throughout the *Mtb* infection cycle in human beings. Multiple *Mtb* antigen-discovery screens studying antigen recognition by blood cells or antibodies from *Mtb* infected individuals have identified antigens encoded by *Mtb* genes highly expressed during *in vivo* infection (IVE-TB antigens) or linked to specific TB infection stages.

To translate these findings towards controlled animal models, we here determined which IVE-TB antigens are recognized by murine T cells following *Mtb* challenge or BCG vaccination. We assessed IFN-γ, TNF-α and IL-17 responses in three different, genetically unrelated mouse strains differing in TB susceptibility, using different experimental settings. Nineteen *Mtb* antigens were recognized across TB resistant and susceptible mice in a first screen, of which 11 were confirmed in infected hypersusceptible C3HeB/FeJ mice. Further corroborating

previous human data, several *Mtb* antigens induced considerable cytokine responses other than IFN-γ. Lung and mediastinal cells from C3HeB/FeJ mice showed a reduced capacity in TNF-α production in response to *Mtb* antigens, agreeing with the TB hypersusceptibility phenotype. In addition, the recently discovered IVE-TB antigen Rv0470 as well as two additional antigens (Rv1733 and Rv3616) were recognized also by splenocytes from C3HeB/FeJ mice immunized with BCG. We conclude that recognition of several promising *Mtb* antigens identified in humans validates across multiple mouse TB infection models with widely differing TB susceptibilities. This offers new translational tools to evaluate IVE-TB antigens as TB diagnostics and TB vaccine antigens in appropriate animal models.

4

INTRODUCTION

Tuberculosis (TB) remains the most widespread and deadly infectious disease from a single pathogen worldwide (1). The transmission of its causative agent, *Mycobacterium tuberculosis* (*Mtb*), cannot be sufficiently controlled -in adolescents and adults- by childhood vaccination with Bacillus Calmette-Guérin (BCG), the only currently licensed TB vaccine (2). Therefore, numerous efforts in the last decades have attempted to develop better TB vaccines (3). Two recent and independent clinical efficacy trials showed that BCG re-vaccination led to a decrease in sustained *Mtb* infection, and that multiple injections of an adjuvanted TB subunit vaccine, M72/AS01E, were able to prevent development of TB in latently *Mtb* infected individuals (4, 5). Although the efficacy of M72/AS01E still needs to be corroborated in larger cohorts and across different geographical areas (6), this finding underscores the clear potential of using selected *Mtb* antigens as BCG booster vaccines (2). However, immune correlates of TB protection remain unknown, posing a challenge to the identification of such protective *Mtb* antigens for vaccine design (7).

In recent years, we have identified a new class of *Mtb* antigens, named IVE-TB antigens, encoded by *Mtb* genes that are highly and consistently expressed in the lung of TB susceptible (C3HeB/FeJ) as well as TB resistant (C57BL/6J) mice following aerosol *Mtb* (Erdman) challenge (8, 9). Because these *Mtb* genes are highly expressed *in vivo*, the encoded IVE-TB proteins represent an interesting set of candidate antigens for several reasons. First of all, they are preserved among at least 219 *Mtb* clinical isolates and other pathogenic mycobacteria, thus offering the potential to elicit immune responses against multiple human virulent *Mtb* strains. Secondly, they share high homology with BCG and are thus likely implementable in booster vaccine strategies. Additionally, they contain multiple predicted HLA-Ia and HLA-II binding motifs covering 85% of the human population. Lastly but most importantly, many IVE-TB antigens were found to be recognized by immune cells of latently *Mtb* infected (LTBI) subjects and TB patients (9, 10). Interestingly, these T cells were capable of producing multiple cytokines, in addition to or even in the absence of IFN-γ, a cytokine known to be necessary but not sufficient in conferring protection against TB (9, 10).

Due to the absence of human *Mtb* challenge models and validated correlates of protection, promising candidate vaccines are commonly tested in mice before being evaluated in larger animal models and eventually clinical trials (11). Many *Mtb* antigens, such as those included in the most advanced candidates in the TB vaccine pipeline (12-16), have been screened previously in C57BL/6 and BALB/c (17). Both strains (particularly C57BL/6) are relatively resistant to TB and do not display the full

spectrum of human TB pathology, such as the development of centrally necrotic lesions (18). By contrast, the less frequently used C3HeB/FeJ strain (also known as the Kramnik model) presents with necrotic lesions and lung cavitation resembling those found in human TB (19).

In order to translate our previous findings from human cohorts towards highly controlled experimental *in vivo* TB models in which protective efficacy of candidate vaccines can be explored, we aimed to: (I) evaluate promising IVE-TB antigens across different strains of *Mtb* infected mice, including not only TB resistant (C57BL/6, BALB/c), but also TB susceptible (C3HeB/FeJ) strains, reasoning that the recognition of antigens in mice with different genetic backgrounds, and widely different TB susceptibilities, would better reflect the TB heterogeneity found in the human population; (II) study whether IVE-TB antigens induce IFN-γ as well as non-IFN-γ cytokine responses (TNF-α and IL-17) also in mice and in different organs (i.e., spleen, lung and mediastinal draining lymph nodes), to enable identification of those antigens that, though recognised in all mouse strains, would induce different cytokines profiles in resistant and susceptible mice. Upon asserting that an antigen is recognised in the susceptible strain, the cytokine and cellular responses can then be redirected towards a protective response (e.g., the response found in the resistant strains) by vaccination using appropriate adjuvants. (III) To determine which IVE-TB antigens recognized during *Mtb* infection are also recognized following vaccination with BCG, with the rationale to discriminate between highly specific *Mtb* antigens that could be useful candidates for TB diagnostics in areas with standard neonatal BCG vaccination programs, versus *Mtb*/BCG shared antigens that can be used as BCG booster vaccines; (IV) and validate findings in a multi-laboratory approach across two different laboratories and experimental settings to strengthen confidence in the results, especially in light of the large heterogeneity distinctive of human TB. The latter conforms to recent recommendations, which encourage researchers to perform pre-clinical discovery screenings in different mouse strains, routes of infection, *Mtb* strains and laboratories, before moving to more costly and resource demanding animal and human studies (17).

We find nineteen *Mtb* antigens that are significantly recognized by cells isolated from different murine tissues, presenting a wide array of immune responses with respect to the cytokines produced and the three mouse genetic backgrounds investigated. Of note, the recognition of eleven of these antigens was corroborated in an independent setting. Thus, our multi-laboratory approach identified new promising *Mtb* antigenic targets for potential application as tools in TB control.

MATERIALS AND METHODS

Intratracheal *Mtb* infection in C57BL/6, BALB/c and C3HeB/FeJ. C57BL/6, BALB/c and C3HeB/FeJ mice were bred in the animal facilities of Sciensano. Mice or breeding couples were obtained from Janvier Labs (France) for C57BL/6 and BALB/c or from The Jackson Laboratory (USA) for C3HeB/FeJ (JAX stock #000658). Aged-matched female mice 8-15 weeks old at the start of each experiment were used. All *Mtb* infections were performed in a biosafety level three (BSL3) facility at Sciensano and all the procedures were performed in accordance with the Belgian legislation and were approved by the ethics committee of Sciensano under the file number 201405-14-01.

Mice were infected intra-tracheally with a dose of 1×10^4 CFU of virulent and luminescent *M. tuberculosis* H37Rv grown for two weeks as a surface pellicle on Sauton medium and stored frozen in aliquots at −80°C. The *M. tuberculosis* H37Rv strain used is transformed with the reporter plasmid pSMT1, which expresses the *Vibrio harveyi luxAB* genes under the control of the BCG hsp60 promoter (20). We have previously shown that measuring RLU is an accurate alternative to determining CFU counts (20, 21). Bacterial loads in total lungs of infected mice were verified at the specified time-points in all infected mice for the first screen. For the second and third screens, bacterial loads were measured in the left lung lobe of individual mice of one pool/time-point. The other lobes and total lungs of the mice of the other pools were treated with Collagenase/DNAse I for isolation of leukocytes. To measure bacterial loads, the number of bioluminescent organisms [determined as relative light units (RLU)] in lung homogenates was determined by a bioluminescence assay with a Modulus luminometer (Turner Biosystems) and 1% n-decanal in ethanol as a substrate. Data are expressed as mean log10 mRLU values per group (Supplementary Data 1).

Preparation of cells harvested from intratracheal *Mtb* infected C57BL/6, BALB/c and C3HeB/FeJ mice. Uninfected naïve control mice and infected mice were sacrificed at specified time-points (Supplementary Data 1). Spleens, lungs and mediastinal lymph nodes were removed aseptically and prepared for cell culture. For that purpose, spleens, mediastinal lymph nodes and lungs (first screen, Supplementary Data 1) were gently homogenized in RPMI medium supplemented with penicillin (60 μg/ml) using a Dounce homogenizer. Mediastinal lymph nodes and lungs (first screen, Supplementary File 1) were passed through a 70 μm nylon cell strainer (Greiner). Lungs (second and third screen, Supplementary Data 1) were fragmented using a scalpel and digested for 1h at 37°C and 5% CO_2 in HBSS (Gibco) supplemented with penicillin (60 μg/ml) and streptomycin (100 μg/ml), 5% of foetal calf serum (FCS), 1 mg/ml of Collagenase from Clostridium histolyticum

(Sigma-Aldrich, C5138) and 0.1 mg/ml of DNAse I from bovine pancreas (Roche, 11284932001). After incubation, digested lung fragments were gently homogenized in a Dounce homogenizer and passed through a 70 µm nylon cell strainer (Greiner). Single cell solutions of cells isolated from spleen, mediastinal lymph nodes and lungs were washed, counted and cultured in RPMI medium supplemented with 5×10^{-5}M 2-mercaptoethanol, penicillin (60 µg/ml) and streptomycin (100 µg/ml), and 10% FCS (number of cells in Supplementary Data 1). Cells isolated from the same organ and mouse strain were pooled in order to have a sufficient number of leukocytes. Pools of cells isolated from 4-13 organs/experimental group were cultured for 72h with recombinant proteins (10 µg/ml) or RPMI as a negative control (defined as unstimulated samples) or Pokeweed (PWM, 20 µg/ml, Sigma, Cat. N° L9379) or Concanavalin A (ConA, 4 µg/ml, Sigma, Cat. N° C5275) as positive controls. Cell free culture supernatants from at least three separate wells were pooled and supernatants were stored frozen at −20 °C until analysis by enzyme-linked immunosorbent assay (ELISA) was performed.

Intranasal *Mtb* infection and sub cutaneous BCG vaccination of C3HeB/FeJ. C3HeB/FeJ female mice purchased from the Jackson Laboratory (USA, JAX stock #000658) were used in this study at six weeks of age. C3HeB/FeJ mice were infected with 1×10^5 CFU live *Mtb* strain H37Rv from glycerol stocks, stored at -80°C. Mice were anesthetized with 2-chloro-2-(difluoromethoxy)-1,1,1-trifluoro-ethane (isofluoran; Pharmachemie BV, The Netherlands) and intranasally (i.n.) infected. Six weeks post *Mtb* challenge, mice were euthanized with CO2 and lungs and splenocytes were aseptically removed. Organs were homogenized using 70 µM cell strainers (Corning, U.S.A.) and the amount of *Mtb* bacteria was determined by plating out serial dilutions of the homogenates on 7H11 plates (BD Bioscience, U.S.A), supplemented with BBL Middlebrook OADC enrichment (BD Bioscience, U.S.A) and PANTA (BD Bioscience, U.S.A). Colonies were counted after three weeks of incubation at 37°C (Supplementary File 2). For BCG immunization, C3HeB/FeJ mice were injected subcutaneously in the right flank with 10^6 CFU BCG1331 (SSI, Denmark) from glycerol stocks, stored at -80°C. Six weeks post BCG vaccination, mice were sacrificed and splenocytes were aseptically removed. Naïve mice were included as control. All mice were daily monitored for ethical requirements, and weighed once a week according to the ethical regulations at the LUMC animal facility (DEC number 11183).

Recombinant proteins. A total of 27 *Mtb* recombinant proteins, previously identified by different *Mtb* antigen discovery approaches (3), were tested in this study (Table 1). As described previously (9), *Mtb* genes as well as the HPV16E6 gene, were amplified by PCR from genomic H37Rv DNA and cloned by Gateway technology (Invitrogen, Carlsbad, CA, USA) in a bacterial expression vector, overexpressed in *Escherichia*

Table 1. List of *Mtb* antigens included in this study.

List	Rv number	Gene name	Category	Reference(s)
1	Rv0287/Rv0288	EsxG/EsxH	IVE-TB	Coppola 2016
2	Rv0440	GroEL2	IVE-TB	Coppola 2016
3	Rv0470c	PcaA	IVE-TB	Coppola 2016
4	Rv0642c	MmaA4	IVE-TB	Coppola 2016
5	Rv0826	Conserved hypothetical protein	IVE-TB/ latency antigen	Coppola 2016; Rustad 2008
6	Rv0991	Conserved serine rich protein	IVE-TB	Coppola 2016
7	Rv1131	PrpC	IVE-TB	Coppola 2016
8	Rv1221	SigE	IVE-TB	Coppola 2016
9	Rv1791	PE19	IVE-TB	Coppola 2016
10	Rv1846	BlaI	IVE-TB	Coppola 2016
11	Rv1872	IldD2	IVE-TB	Coppola 2016
12	Rv1980c	Mpt64	IVE-TB	Coppola 2016
13	Rv2461	ClpP1	IVE-TB	Coppola 2016
14	Rv2626	Hrp1	IVE-TB/ latency antigen	Coppola 2016; Commandeur 2011; Serra-Vidal 2014
15	Rv2873	Mpt83	IVE-TB	Coppola 2016
16	Rv3048c	R1F protein	IVE-TB	Coppola 2016
17	Rv3052	FadB4	IVE-TB	Coppola 2016
18	Rv3583c	Possible transcription factor	IVE-TB	Coppola 2016
19	Rv3615	EspC	IVE-TB	Coppola 2016
20	Rv3616*	EspA	IVE-TB	Coppola 2016
21	Rv3846	SodA	IVE-TB	Coppola 2016
22	Rv3874/Rv3875	ESAT6/CFP10 (E/C)	IVE-TB/secreted antigens	Van Pinxteren 2000; Coppola 2016
23	Rv1733c	Rv1733c	latency antigen	Commandeur 2011; Serra-Vidal 2014
24	Rv2034	Rv2034	IVE-TB stage specific	Commanduer 2013
25	Rv3353c	Rv3353c	IVE-TB stage specific	Commanduer 2013
26	Rv2029c	Rv2029c	latency antigen	Commandeur 2011; Serra-Vidal 2014
27	Rv1886c	Ag85B	secreted antigens	Babaki 2017

Previously described immunodominant *Mtb* specific antigens are shown in bold font; *patent WO 2014063704 A2. Definitions of abbreviations: *Mtb* = *Mycobacterium tuberculosis*; IVE-TB = *in vivo* expressed *Mtb* antigens. Gene names were reported according to their annotations in the Mycobrowser data repository (https://mycobrowser.epfl.ch/).

coli (*E. coli*) BL21 (DE3) and purified. Gel electrophoresis and western blotting with an anti-His tag Antibody (Invitrogen) and an anti-*E. coli* polyclonal antibody (a kind gift of Statens Serum Institute, Copenhagen, Denmark) were used to check the size and purity of the recombinant proteins. Rv0287/88 and Rv3874/75 were produced as fusion proteins to mirror the pairwise dependent secretion pathway by the mycobacterial T7S system. All recombinant proteins here included were previously tested to confirm lack of protein-nonspecific T-cell stimulation and cellular toxicity (9).

ELISA on cells harvested from intratracheally *Mtb* infected mice. IFN-γ was quantified by sandwich ELISA using purified rat anti-mouse IFN-γ clone R4-6A2 (BD Biosciences, Cat. N° 551216) as the capture antibody, biotinylated rat anti-mouse IFN-γ clone XMG1.2 (BD Biosciences, Cat. N° 554410) as detection antibody, peroxidase-conjugated streptavidin (Jackson ImmunoResearch, Cat. N° 016-030-084) and recombinant mouse IFN-γ protein (R&D Systems, Cat. N°485-MI) as standard. Plates were revealed with O-phenylenediamine dihydrochloride substrate (SIGMAFAST™ OPD, Cat. N° P9187), the reaction was stopped with 1 M H_2SO_4, and the optical density was read at 490 nm on an Infinite F50 plate-reader (Tecan).

TNF-α and IL-17A were quantified by sandwich ELISA with respectively TNF-α mouse uncoated ELISA kit (Invitrogen, Cat. N° 88-7324-88) and IL-17A (homodimer) mouse uncoated ELISA kit (Invitrogen, Cat. N° 88-7371-88) following the recommended manufacturer's procedures and optical density was read at 450 nm on an Infinite F50 plate-reader (Tecan).

The respective dynamic ELISA assay ranges are 20-5000 pg/mL for IFN-γ; 8-1000 pg/mL for TNF-α and 4-500 pg/mL for IL-17A and appropriate serial dilutions of the samples were tested to quantify these three different cytokines.

ELISA results were analysed by converting measured absorbance to concentrations (pg/ml) by linear regression of the optical densities measured for the diluted standards using the Magellan for F50 software (Tecan).

ELISA on samples form intranasally *Mtb* infected and subcutaneously BCG vaccinated mice. *Mtb* infected splenocytes (300,000 cells/well) were incubated with single recombinant proteins or mitogens (5 μg/ml) at 37°, 5% CO2. After six days of stimulation, the supernatants were filtered through 0.2 μM filter plates (Corning, U.S.A.). The IFN-γ ELISA (BD Bioscience, U.S.A, capture antibody cat no 551216 and biotin labelled detection antibody cat no 554410) was performed on the filtered supernatants according to manufacturer's instructions. Absorbance (OD450) was determined and converted to concentrations using a standard curve by the

Microplate Manager software version 5.2.1 (Biorad Laboratories, The Netherlands) (Supplementary Data 2).

Data analysis. For each cytokine, within each pool of mice (Supplementary Data 1) or single mouse (Supplementary Data 2), the background-value, i.e., the value determined for unstimulated samples, was subtracted from the value determined for each antigen or mitogen. Data obtained at the later stage are pooled for analysis (9-12 wks). The Kruskal-Wallis test was performed to assess the difference between the responses found in uninfected mice versus infected mice at different time points or versus BCG immunized mice for each antigen using IBM SPSS Statistics 26 (Supplementary Data 1 and 2). Due to the high number of comparisons included in the study, we performed a two-sided Mann-Whitney test with an FDR (Benjamini-Hochberg) correction (results reported in the Supplementary Data 1 and 2). However, significant responses to positive controls or to previously described antigens (such as ESAT6/CFP10) were lost after correction (with an FDR cut-off set at 0.1), questioning whether this more stringent approach could lead to the exclusion of interesting candidates at this early stage of discovery. Thus, results of both unadjusted and adjusted tests are reported. In addition, for the first set of experiments, we analysed the responses to specific antigens on the basis of known classes ((I) naïve mice vs. mice sacrificed at early or late point after *Mtb* infection; (II) mouse strains; (III) organs; (IV) cytokines) using a supervised partial least squares-discriminant analysis (PLS-DA) method (Supplementary Figure 2A) and a principal component analysis (PCA) (Supplementary Figure 2B). The median responses to each specific antigen (Supplementary Data 1) were explored and analysed with 'mixOmics' (package version 6.15, http://www.mixOmics.org) in R (version 4.0.3) after log10 transformation. Three-component models explained the highest proportion of variance in the PCA as well as lowest balanced error rate (BER) in the PLSA-DA (Supplementary Data 1). For each of the categories investigated through PLSA-DA, we obtained Variable Importance in Projection (VIP) values which are a quantitative estimation of the discriminatory power of each individual antigen in a specific model (Supplementary Data 1). The VIP values vary in a fixed range since the sum of squared VIP scores for all variables sum to the number of variables (22). Therefore, antigens with a VIP value larger than 1 (i.e., larger than the average of squared VIP values) were considered to have an above average influence on the model (22).

The Kruskal-Wallis test with Dunn's multiple test correction was applied in Graphpad Prism (version 8) to analyse cytokine responses measured for all the 27 *Mtb* antigens across organs and timepoints (Supplementary Figure 1).

Of note, in the second experiment, the IFN-γ response to HPV16E6, used as negative control, was higher in mice after BCG or *Mtb* infection than in the uninfected group. This response could be due to a non-specific immune activation profile. Therefore, we considered responses to be significant and specific only when the median IFN-γ production exceeded twice the IFN-γ production found in response to the negative control in BCG immunized and *Mtb* infected mice.

Data availability. All data generated or analysed during this study are included in this published article and its supplementary information files: Supplementary Data 1 and Supplementary Data 2, which are available online at: https://www.nature.com/articles/s41541-021-00343-2#MOESM3.

Code availability statement. The code used in this study was obtained from the 'mixOmics' (package version 6.15, http://www.mixOmics.org) for R (version 4.0.3).

4

RESULTS

IVE-TB antigen recognition in multiple organs of three genetically different mouse strains by cells producing different cytokines.

Promising TB candidate vaccine antigens first need to be validated in small animal models before they can be selected for evaluation in larger animal models such as non-human primates, and eventually for testing in human clinical trials (11). Here, we aimed to verify which IVE-TB antigens, previously shown to be recognized by T cells from TB patients and LTBI subjects (9, 10), were consistently and broadly recognized during the course of murine *Mtb* infection in different genetic backgrounds, given the fact that human populations are genetically highly diverse. To include different genetic backgrounds with widely diverse TB susceptibility phenotypes, we selected C57BL/6, BALB/c and C3HeB/FeJ mice and challenged these with *Mtb* (20, 23). Different cell pools from each organ (spleens, lungs and mediastinal lymph nodes (medLN)), strain and time-points (early (five weeks) or later (9-12 weeks) stage of *Mtb* infection) were tested in parallel by stimulation with single or fusion IVE-TB antigens (n=22) (Table 1) as well as with positive controls (ConA and PWM) (Figure 1A, Supplementary Data 1). Besides IVE-TB antigens, also several other, stage specific- and secreted-*Mtb* antigens (n=five) were included in the screening since several studies previously described these as promising (diagnostic) TB biomarkers or as putative antigens for TB vaccination (24-27) (Table 1). The concentrations of IFN-γ, TNF-α and IL-17 were measured in the cell supernatants after 3 days of stimulation. Cytokine levels in response to each *Mtb* antigen were compared between naïve mice and *Mtb*
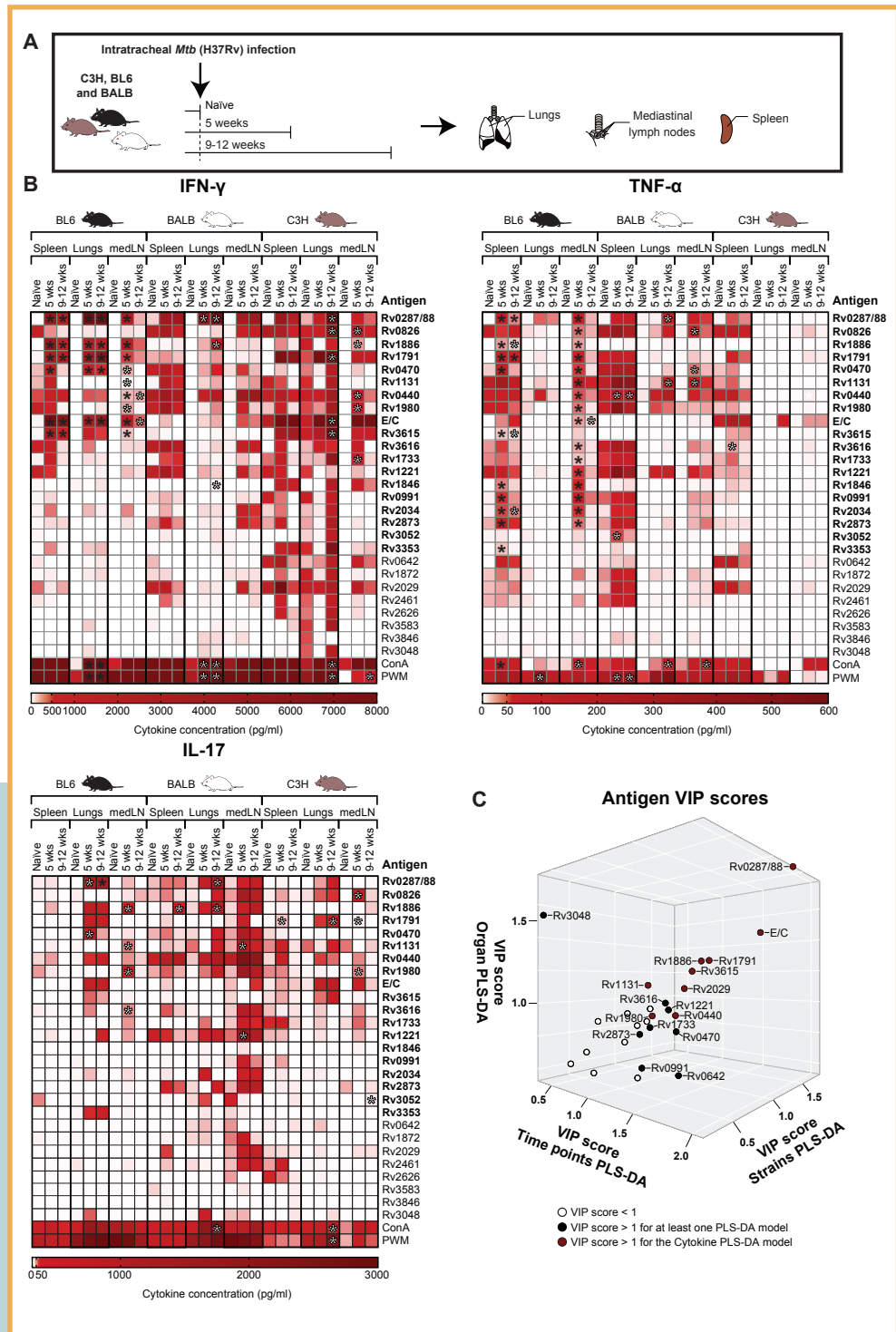
challenged mice for each organ and mouse strain, after subtracting background concentrations from unstimulated negative control samples (Supplementary Data 1).

Several trends emerged when grouping the cytokine responses against the 27 *Mtb* antigens included in this study (Supplementary Figure 1). High TNF-α responses were found to the majority of the selected *Mtb* antigens, most predominantly in the spleen, in all three mouse strains. Secondly, the cells analysed from the C3HeB/FeJ mice showed an overall reduced ability to produce TNF-α against *Mtb* antigens, especially cells from the medLN and lungs whose TNF-α response was low or absent even after mitogen stimulation (Figure 1B, Supplementary Figure 1). Antigen specific IFN-γ and IL-17 responses were more diversely distributed and varied strongly between organs and mouse strains (Figure 1B). Interestingly, especially in BALB/c and C57BL/6 mice, significant IL-17 responses were mainly induced in cells isolated from the lungs and medLN, while IL-17 responses were almost absent among the splenocytes (Supplementary Figure 1). For splenocytes and medLN, the highest peak of cytokine production was mostly observed at an early stage of *Mtb* infection, while for lung cells this was observed at the later stage (Supplementary Figure 1). IFN-γ responses tended to be highest in C3HeB/FeJ mice, the most TB susceptible strain, confirming that like in humans IFN-γ in itself is not sufficient for protective immunity.

Among the *Mtb* antigens that induced a significant specific increase in cytokine production, the highest number was recognized by medLN cells from C57BL/6 mice

4

Figure 1. Most IVE-TB antigens are recognized by cells from *Mtb* infected mice with differences among mouse strains, organs and cytokines. (A) C57BL/6 (BL6), BALB/c (BALB) and C3HeB/FeJ (C3H) mice were challenged with 1x10^4 CFU *Mtb*-lux strain intratracheally and sacrificed at an early (five weeks) or later (9-12 weeks) stage of *Mtb* infection. Uninfected naïve control mice were sacrificed and tested in parallel. Pooled cells from lungs, mediastinal lymph nodes (medLN) or spleens were stimulated with single or fusion *Mtb* antigens or with positive control stimuli ConA and PWM. The concentrations of IFN-γ, TNF-α and IL-17 were measured in the cell supernatants after three days of stimulation and corrected for background. (B) Heatmaps of the specific *Mtb* antigen responses for each cytokine are shown. Colour gradients indicate the cytokine concentration, while asterisks indicate significant differences between the naïve and the *Mtb* challenged groups. White *: p-value<0.05, computed with Kruskal-Wallis test; black * marks differences that remained significant after multiple test correction (q-value <0.1, i.e., FDR-adjusted p-values of Mann-Whitney test). (C) 3-D plot of the Variable Importance in Projection (VIP) scores obtained from each PLS-DA model computed on the basis of the following known classes: (I) time points (i.e., naïve mice vs. mice sacrificed at early or late point after *Mtb* infection); (II) mouse strains (i.e., C57BL/6 (BL6), BALB/c (BALB) and C3HeB/FeJ (C3H) mice); (III) organs (i.e., lungs, mediastinal lymph nodes or spleens); (IV) cytokines (i.e., IFN-γ, TNF-α and IL-17). Antigens with a VIP score > 1 were considered to have an above average influence on the model and are depicted by solid dots. Antigens with a VIP score > 1 for the cytokine PLS-DA model are depicted by solid red dots. Antigens with a VIP score < 1 are depicted by empty dots and their names are omitted in the 3D plot.

(18/27 antigens recognized), followed by C3HeB/FeJ (7/27 antigens recognized) and BALB/c (4/27 antigens recognized) mice (Figure 1B). From these antigens, only one was recognized by all mouse strains (Rv0826), five by C57BL/6 and C3HeB/FeJ (Rv1886, Rv0440, Rv1980, Rv1791, and Rv1733), and three by C57BL/6 and BALB/c mice (Rv1131, Rv1221, and Rv0470). In the C57BL/6 mice and, to a lesser extent, in the other two mouse strains, medLN cells produced multiple cytokines in response to single *Mtb* antigens. The different combinations found were: IFN-γ, TNF-α and IL-17 against three antigens (in C57BL/6 mice: Rv1886, Rv1131 and Rv1980); IFN-γ and TNF-α against five antigens (in C57BL/6 mice: Rv0287/88, Rv0470, Rv1791, ESAT6/CFP10 and Rv0440. For Rv0440, the same cytokine profile was found in C3HeB/FeJ mice); IFN-γ and IL-17 against two antigens (in C3HeB/FeJ mice: Rv0826 and Rv1980); TNF-α and IL-17 against two antigens (in C57BL/6 mice: Rv3616; in BALB/c mice: Rv1131).

Antigen-specific splenocyte responses to *Mtb* antigens were mainly detected-as measured by either one or more of the three cytokines evaluated- in C57BL/6 mice (11 antigens recognized) and to a lesser extent in BALB/c (three antigens recognized) and C3HeB/FeJ (two antigens recognized) mice. Among these, only the recognition of one antigen, Rv1886, was shared between C57BL/6 and BALB/c mice, and one other (Rv1791) between C57BL/6 and C3HeB/FeJ. Only splenocytes from C57BL/6 mice produced multiple cytokines, i.e., IFN-γ and TNF-α, against five antigens (Rv1886, Rv0287/88, Rv0470, Rv1791, and Rv3615).

Lung cells consistently recognized fewer antigens than cells isolated from other tissues (Figure 1C). However, some of these antigens were recognized by lung cells of different mouse strains (Rv0287/88 was recognized by all mouse strains; Rv1886 by C57BL/6 and BALB/c; ESAT6/CFP10 and Rv1791 by C57BL/6 and C3HeB/FeJ). Significant levels of IFN-γ and IL-17 were secreted by lung cells in response to four antigens (in C57BL/6 mice: Rv0287/88 and Rv0470; in BALB/c mice: Rv1886; in C3HeB/FeJ mice: Rv1791). Only against one antigen (Rv0287/88) a combined IFN-γ, TNF-α and IL-17 response was found in BALB/c mice.

Most of the differences listed above were no longer significant after the very stringent FDR correction, but importantly this included also responses to controls and to previously described antigens known to be highly immunogenic such as ESAT6/CFP10 (Figure 1B and 2C). Therefore, the results are shown both with and without FDR correction, to avoid the risk of missing biological relevant candidates at this early stage of discovery,

Interestingly, in the resistant mouse strains, there were a few antigens (Rv0470, Rv0826, Rv0991, Rv 1131, Rv1221, Rv1733, Rv1846, Rv1980, Rv2034, Rv2873, Rv3052, Rv3353, and Rv3616) that induced statistically significant TNF-α but not IFN-γ responses. Except for Rv1846, this lack of overall significant IFN-γ responses seemed to be the result of the observed heterogeneity in donor responses rather than the complete absence of this cytokine (Supplementary Figure 3).

To validate the results in a subsequent independent multivariate analytical approach, we used PLS-DA modelling to determine the key antigens that drove the discrimination in cytokine responses between (I) time points (E/C, Rv0642, Rv0287/88, Rv0991, Rv1791, Rv1886, Rv2029, and Rv3616); (II) mouse strains (E/C, Rv0287/88, Rv0440, Rv0470, Rv0642, Rv1221, Rv1791, Rv1886, Rv2029, Rv2873, and Rv3615); (III) organs (E/C, Rv0287/88, Rv1131, Rv1791, Rv1886, Rv2029, Rv3048, Rv3615, and Rv3616); and (IV) type of cytokine (E/C, Rv0287/88, Rv0440, Rv1131, Rv1791, Rv1886, Rv1980, Rv2029, and Rv3615), based on the Variable Importance in Projection (VIP) values (VIP>1). The PLS-DA protein clusters (Supplementary Figure 2A) were very similar to those obtained by unsupervised PCA (Supplementary Figure 2B) confirming their validity. (Supplementary File 1, Figure 1C). Of note, this independent multivariate approach confirmed 13 of the 19 proteins that were found as being interesting targets in our first analysis.

Overall, nineteen out of 27 selected *Mtb* antigens (Figure 1C, in bold) elicited significant cytokine production from cells isolated from *Mtb* infected mice compared to those found in uninfected animals. Of note, although as expected these responses were somewhat heterogeneous, thirteen antigens appeared to drive discriminatory cytokine responses between the different mouse strains, time points, type of cytokine and tissues analysed in this study. But perhaps most importantly, the results show that human T cell recognition profiles translate well to mouse models, which was a major aim of this study.

IVE-TB antigen-specific responses after live BCG vaccination.

A TB subunit vaccine, in order to be effective, should preferably boost immune responses induced by prior vaccination (28). BCG, despite its insufficient protective efficacy against adult TB, remains the only licensed vaccine against TB and is highly effective in protecting against severe childhood TB (2). To evaluate whether immune responses against IVE-TB antigens could be induced by BCG immunization, and to compare those responses to those induced by *Mtb* infection, C3HeB/FeJ mice were either challenged with H37Rv-*Mtb* strain (10^5 CFU) (ten mice), vaccinated subcutaneously with BCG (five mice) or left untreated (five mice) (Figure 2A). After six weeks, splenocytes were harvested and stimulated for six days with a set of
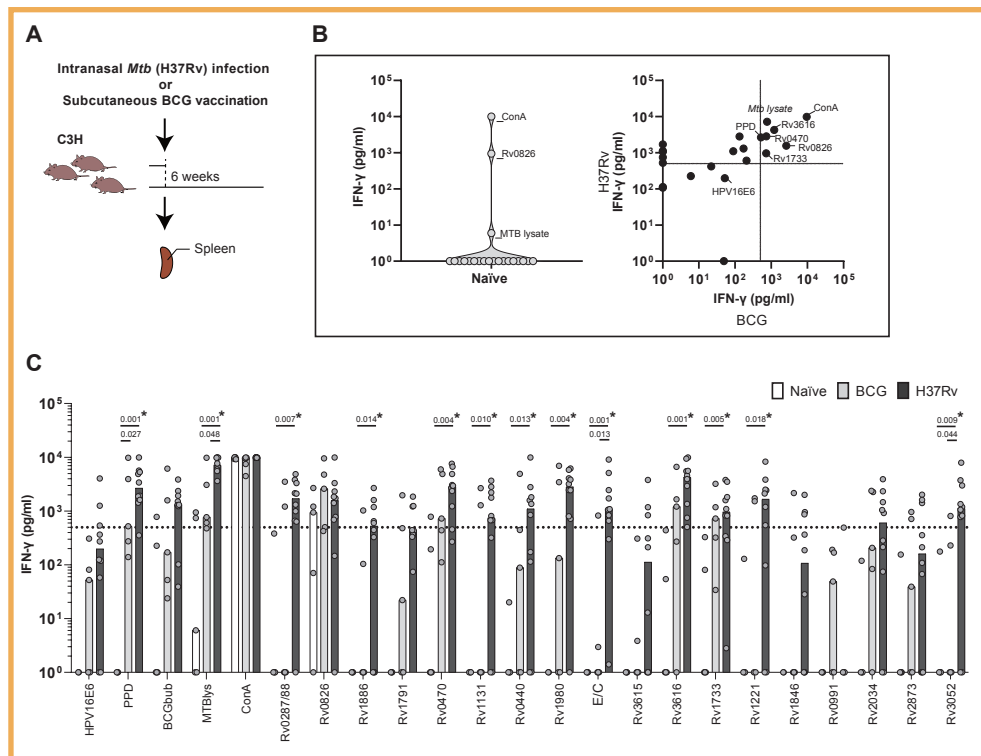
Figure 2. IVE-TB antigen-specific responses after *Mtb* infection and BCG vaccination in C3HeB/FeJ (C3H) mice. (A) C3HeB/FeJ mice were either challenged intranasally with H37Rv-*Mtb* strain (10^5 CFU) (ten mice), vaccinated subcutaneously with BCG (five mice) or left untreated (five mice). After six weeks, splenocytes were harvested and stimulated per mouse for six days with a set of eighteen *Mtb* antigens or positive controls (ConA, PPD, bead disrupted BCG (BCG bub) and *Mtb* lysate), or negative control (HPV16E6 recombinant protein). The IFN-γ concentrations detected in the unstimulated samples were subtracted from the stimulated samples for each condition within each mouse. (B) IFN-γ production after antigen stimulation in splenocytes from naïve unimmunized mice (left panel), and BCG immunized versus *Mtb* infected mice (right panel). Dots display the median IFN-γ production. The (Rv) codes of the antigens are indicated if the median IFN-γ production exceeded 500 pg/ml in both BCG immunized and *Mtb* infected mice. The horizontal dotted line indicates the cut-off at 500 pg/ml, which is twice the median IFN-γ production found in response to the negative control in BCG immunized and *Mtb* infected mice (right panel) (C) IFN-γ responses against *Mtb* antigens in splenocytes from naïve, BCG immunized and *Mtb* infected mice are shown. Dots represent a single mouse (ten mice in the *Mtb* infected group and five mice in the naïve and BCG immunized group in total) and bars indicate the median IFN-γ response of each group. The *Mtb* challenged and BCG immunized groups were compared to the naïve group using the Kruskal-Wallis test and a p-value < 0.05 was considered significant. * marks differences that remained significant after multiple test correction (q-value <0.1, i.e., FDR-adjusted p-values of Mann-Whitney test).

eighteen *Mtb* antigens selected from our first screen (Figure 1C). Positive (ConA, PPD, bead disrupted BCG, *Mtb* lysate) and negative (HPV16E6 recombinant protein) controls were also included. The IFN-γ production in response to the different stimuli was measured and analysed, and, as above, concentrations detected in the unstimulated samples were subtracted from each condition within each mouse. TNF-α and IL-17 responses were only present at low levels in C3H mice in the first experiment (Figure 1B) and therefore not assessed in this screening. Three antigens (Rv0470, Rv1733 and Rv3616) were strongly recognized by *Mtb* infected as well as BCG vaccinated C3HeB/FeJ mice (i.e.: IFN-γ production > 500 pg/ml) (Figure 2B). Additionally, despite the different experimental setup and laboratory setting, eleven *Mtb* antigens (Rv0287/88, Rv1886, Rv0470, Rv1131, Rv0440, Rv1980, ESAT6/CFP10, Rv3616, Rv1733, Rv1221 and Rv3052) were confirmed to be significantly recognised after *Mtb* challenge in C3HeB/FeJ mice (Figure 2C). Interestingly, besides ESAT6/CFP10 (E/C), of which peptides are already widely used as TB diagnostic tool in IGRA tests (29), Rv0287/88, Rv1886, Rv1131, Rv1221, Rv1846, and Rv3052 were the only antigens for which IFN-γ responses differed highly between the *Mtb* infected and the BCG vaccinated group (Figure 2C). Prior to FDR correction, differences between the *Mtb* infected and the BCG vaccinated group were significant only for E/C (as expected), Rv3052 and *Mtb* lysate.

Collectively, these findings confirm, extend and partially validate the immune recognition of eleven *Mtb* antigens previously identified in humans across three genetically unrelated mouse TB infection models and two different independent laboratory settings.

DISCUSSION

An important requirement for novel TB candidate vaccines is that they evoke immunity to *Mtb* proteins that are expressed, processed and presented to the host immune system during infection. Over the last years, we identified multiple *Mtb* proteins recognized by immune blood cells from latently *Mtb* infected individuals and TB patients (3, 9). During the antigen selection process, we selected proteins encoded by genes highly expressed either during the entire course of infection, or during specific stages of *in vivo Mtb* infection (3). Before entering clinical studies, candidate vaccines need to be evaluated and proven to be immunogenic in animal studies (11). Therefore, we here examined a selection of *Mtb* antigens identified in our previous *in vitro* human studies and back translated this to three different, genetically and TB-susceptibility diverse mouse TB models. We found that among a set of 27 *Mtb* antigens recognized by human cells, 19 were able to induce the

production of at least one of three cytokines (IFN-γ, TNF-α, IL-17) in at least one of the tissues examined in each of the three mouse strains after challenge with *Mtb*. Further confirmation of our previous data in human cohorts was that several *Mtb* antigens induced considerable cytokine responses other than IFN-γ (9, 30). Importantly, and in accordance with new recommendations (17), the results were partially validated in a second independent laboratory and experimental setting (Supplementary File 3), showing recognition of 11 *Mtb* antigens in infected C3HeB/FeJ mice. Among those, three antigens (i.e.: Rv0470, Rv1733 and Rv3616) were found to be recognized also after BCG vaccination. The latter finding is essential when considering the design of BCG-booster vaccines against TB (2).

Overall, in the experiments performed in the first laboratory, we observed highly significant responses to *Mtb* antigens which varied by magnitude, cytokine combinatorial patterns, tissues and mouse strains (Figure 1). As previously observed in human studies (9), the differences in the levels and types of cytokines induced by an antigen, or the fact that certain antigens did not elicit detectable immune responses, is not linked to a particular protein function. Interestingly, non IFN-γ responses were detected in the spleen and the mediastinal draining lymph nodes of the resistant C57BL/6 mouse strain after stimulation with a substantial number of antigens (Rv0470, Rv0826, Rv0991, Rv 1131, Rv1221, Rv1733, Rv1846, Rv1980, Rv2034, Rv2873, Rv3353, and Rv3616), which agrees with our previous findings (9) and also with the recent description of non-canonical IFN-γ-independent immune responses found in the peripheral blood of *Mtb* exposed "resistant" individuals (30). Cells from C57BL/6 mice recognized significantly more *Mtb* antigens than those from BALB/c and C3HeB/FeJ mice. Although C57BL/6 and BALB/c mice are equally resistant to TB (31), several genetic determinants might have contributed to the differences found in the antigens recognized. For instance, the adaptive type 1 immune response to pulmonary mycobacterial infection appears later and with lower magnitude in BALB/c compared to C57BL/6 mice (32, 33). In line with our findings, the lower magnitude of IFN-γ and TNF-α production levels in BALB/c mice was already described in splenocytes and lung lymph node cells upon antigen stimulation (33). Unexpectedly to us, we found that lung and mediastinal lymph nodes cells from C3HeB/FeJ mice failed to produce detectable TNF-α, not only after *Mtb* antigens exposure, but also upon some of the positive mitogen controls. During mycobacterial infection, TNF-α deficient mice develop necrotic granulomas, pathogenic lesions which are also characteristic of the C3HeB/FeJ mice (34, 35). Although cells isolated from lung of C3HeB/FeJ mice can produce TNF-α, they do that to a lesser extent than C57BL/6 mice, potentially explaining why they develop necrotic lesions. The lower TNF-α production in C3HeB/FeJ mice might be caused by a greater and premature accumulation of a functionally exhausted T cell subsets, characterized by

a limited capacity to secrete IL-2 and TNF-α (36). Demonstrating the recognition of *Mtb* antigens in this TB susceptible strain was particularly important from a corrective vaccine perspective. Redirecting the cellular response in such strains towards a protective response (e.g., that found in the resistant strain) could be achieved by immunizing mice with recognized antigens and appropriate adjuvants (e.g., CAF01), as has been done for instance with ESAT6 which is a strongly antigenic protein in active TB patients, but is also a powerful antigen for vaccination when delivered in CAF01(37).

Only two antigens were consistently recognized by cells isolated from the same tissue across all mouse strains: Rv0287/88 and Rv0826. Rv0287/88 is a heterodimer secreted by the ESX-3 secretion system, implicated in *Mtb* virulence and survival (38, 39). Lung cells from all three mouse models produced IFN-γ when stimulated with Rv0287/88, while TNF-α and IL-17 were secreted concomitantly in BALB/c mice and TNF-α in C57BL/6 mice. In the latter strain, also splenocytes and mediastinal lymph nodes cells responded to Rv0287/88 by producing IFN-γ and TNF-α. These findings validate and extend what has been shown for lung T cells of CB6F1 (BALB/c x C57BL/6) and B6C3F1 (C57BL/6 × C3HeB/FeJ), which are able to recognize Rv0287/88 after 21 days of *Mtb* infection (40). Although evidence for the antigenicity of Rv0287/88 accumulates, susceptible C3HeB/FeJ mice immunized with BCG did not recognize this fusion protein. This contrasts with another study, performed in a TB resistant strain, wherein splenocytes of BCG vaccinated mice responded to specific Rv0288 epitopes (41). Rv0288 constitutes part of the H4:IC31, an adjuvanted polyprotein vaccine that, though immunogenic, failed to boost neonatal BCG vaccination in a recent prevention of (sustained) infection clinical trial (4). Testing this vaccine in BCG immunized mice with different TB susceptibility phenotypes might provide improved models that are more predictive of humans.

At an early stage of *Mtb* infection, Rv0826 was recognized by medLN cells from all mice, mainly inducing TNF-α in C57BL/6 and BALB/c mice and IFN-γ and IL-17 in C3HeB/FeJ mice. Rv0826 is a conserved protein with unknown function, highly expressed during enduring hypoxia and in extensively drug resistant *Mtb* strains (42, 43). These characteristics, together with the strong cellular recognition found in humans (44) and in mice, would make this antigen an attractive target. However, we observed consistent unspecific immune responses against Rv0826 in the splenocytes of all mice, verified in an independent experiment (Figure 2B), which deserves further investigation. This might be due to cross reactivity to other microbial antigens, e.g., microbiota derived, but this remains currently speculative.

Besides Rv0287/88 and Rv0826, other antigens were consistently recognized across tissues and mouse strains, and better able to elicit cells producing multiple cytokines (Rv1886, Rv1791, Rv0470, Rv1131, Rv0440, Rv1980) than other antigens (ESAT6/CFP10, Rv3615, Rv3616, Rv1733, Rv1221, Rv1846, Rv0991, Rv2034, Rv2873, Rv3052, and Rv3353). Among those, Rv0470c was particularly interesting because it is a novel antigen consistently recognized across mice both after *Mtb* challenge and after BCG vaccination, in independent experiments and in different laboratories. Additionally, though recognized in susceptible mice, Rv0470 induced different magnitudes and type of cytokine responses in the resistant strains (Figure 1b and 1C). Rv0470c is an enzyme essential for both the synthesis and cyclopropanation of mycolic acids and the cording morphology of both BCG and *Mtb* (45, 46). In addition, Rv0470c prevents phagosome maturation in human monocyte-derived macrophages, while in mice, its deletion alters the persistence and pathology of *Mtb* at late stages of infection (45, 47). Of note, immunization with BCG_0470 increased the delayed-type hypersensitivity as well as Th1 responses in BCG primed BALB/c mice (48). All these features, supported by our data in mice and humans (9, 10), point to Rv0470c as an attractive BCG booster vaccine candidate when delivered with a properly selected adjuvant (49).

Interestingly, Rv0287/88, Rv1886, Rv1131, Rv1221, Rv1846 and Rv3052, though highly homologous to M. bovis proteins, were the antigens, besides ESAT6/CFP10, for which IFN-γ response highly differed between *Mtb* infected and BCG vaccinated groups (Figure 2C) (9). Comparing the specific responses between TB patients and non *Mtb* exposed BCG vaccinees might reveal the potential of these antigens as adjunct TB diagnostic tools.

In conclusion, this study, to our knowledge for the first time, demonstrates the consistent recognition of several promising IVE-TB *Mtb* antigens across multiple genetically and TB susceptibility diverse *Mtb* infected mouse strains, across various infection models and tissues and time points evaluated, thus offering new translational tools to evaluate *Mtb* antigens in appropriate animal models.

ACKNOWLEDGEMENTS

AUTHOR CONTRIBUTION

M.C., A.G., M.R. and T.H.M.O: designed the study; M.C.: performed the data analysis; T.H.M.O: gave insights on the analysis; K.L.M.C.F: performed the production and the purification of recombinant proteins; F.J.: performed the experiments shown in Figure 1 and in the Supplementary Figure 1; H.G.T.: contributed to experiments shown in Figure 1; S. J. F. van den E.: performed the experiment shown in Figure 2; AG: supervised the experiment shown in Figure 2; M. R.: supervised the experiments shown in Figure 1 and in the Supplementary Figure 1; M.C. and T.H.M.O: wrote the original draft and subsequent revised versions; A.G. and M.R.: reviewed and edited the manuscript.

COMPETING INTERESTS

The authors declare that there are no competing interests.

4

REFERENCES

1. WHO. World Health Organization: Global tuberculosis report 2019. 2019.
2. Schrager LK, Vekemens J, Drager N, Lewinsohn DM, Olesen OF. The status of tuberculosis vaccine development. The Lancet Infectious diseases. 2020;20(3): e28-e37.
3. Coppola M, Ottenhoff TH. Genome wide approaches discover novel *Mycobacterium tuberculosis* antigens as correlates of infection, disease, immunity and targets for vaccination. Seminars in immunology. 2018; 39:88-101.
4. Nemes E, Geldenhuys H, Rozot V, Rutkowski KT, Ratangee F, Bilek N, et al. Prevention of *M. tuberculosis* Infection with H4:IC31 Vaccine or BCG Revaccination. The New England journal of medicine. 2018;379(2):138-49.
5. Tait DR, Hatherill M, Van Der Meeren O, Ginsberg AM, Van Brakel E, Salaun B, et al. Final Analysis of a Trial of M72/AS01E Vaccine to Prevent Tuberculosis. The New England journal of medicine. 2019;381(25):2429-39.
6. Ottenhoff THM. A Trial of M72/AS01E Vaccine to Prevent Tuberculosis. The New England journal of medicine. 2020;382(16):1576-7.
7. Zhu B, Dockrell HM, Ottenhoff THM, Evans TG, Zhang Y. Tuberculosis vaccines: Opportunities and challenges. Respirology (Carlton, Vic). 2018;23(4):359-68.
8. Commandeur S, van Meijgaarden KE, Prins C, Pichugin AV, Dijkman K, van den Eeden SJ, et al. An unbiased genome-wide *Mycobacterium tuberculosis* gene expression approach to discover antigens targeted by human T cells expressed during pulmonary infection. Journal of immunology (Baltimore, Md : 1950). 2013;190(4):1659-71.
9. Coppola M, van Meijgaarden KE, Franken KL, Commandeur S, Dolganov G, Kramnik I, et al. New Genome-Wide Algorithm Identifies Novel In-Vivo Expressed *Mycobacterium tuberculosis* Antigens Inducing Human T-Cell Responses with Classical and Unconventional Cytokine Profiles. Scientific reports. 2016; 6:37793.
10. Coppola M, Villar-Hernandez R, van Meijgaarden KE, Latorre I, Muriel Moreno B, Garcia-Garcia E, et al. Cell-Mediated Immune Responses to *in vivo*-Expressed and Stage-Specific *Mycobacterium tuberculosis* Antigens in Latent and Active Tuberculosis Across Different Age Groups. Frontiers in immunology. 2020; 11:103.
11. Kaufmann SHE, Dockrell HM, Drager N, Ho MM, McShane H, Neyrolles O, et al. TBVAC2020: Advancing Tuberculosis Vaccines from Discovery to Clinical Development. Frontiers in immunology. 2017;8:1203.
12. Skeiky YA, Alderson MR, Ovendale PJ, Guderian JA, Brandt L, Dillon DC, et al. Differential immune responses and protective efficacy induced by components of a tuberculosis polyprotein vaccine, *Mtb*72F, delivered as naked DNA or recombinant protein. Journal of immunology (Baltimore, Md: 1950). 2004;172(12):7618-28.
13. Ryter KT, Ettenger G, Rasheed OK, Buhl C, Child R, Miller SM, et al. Aryl Trehalose Derivatives as Vaccine Adjuvants for *Mycobacterium tuberculosis*. J Med Chem. 2020;63(1):309-20.
14. Brandt L, Elhay M, Rosenkrands I, Lindblad EB, Andersen P. ESAT-6 subunit vaccination against *Mycobacterium tuberculosis*. Infection and immunity. 2000;68(2):791-5.
15. Aagaard C, Hoang T, Dietrich J, Cardona PJ, Izzo A, Dolganov G, et al. A multistage tuberculosis vaccine that confers efficient protection before and after exposure. Nature medicine. 2011;17(2):189-94.
16. Kwon KW, Lee A, Larsen SE, Baldwin SL, Coler RN, Reed SG, et al. Long-term protective efficacy with a BCG-prime ID93/GLA-SE boost regimen against the hyper-virulent *Mycobacterium tuberculosis* strain K in a mouse model. Scientific reports. 2019;9(1):15560.

17. Franzblau SG, DeGroote MA, Cho SH, Andries K, Nuermberger E, Orme IM, et al. Comprehensive analysis of methods used for the evaluation of compounds against *Mycobacterium tuberculosis*. Tuberculosis (Edinburgh, Scotland). 2012;92(6):453-88.

18. Singh AK, Gupta UD. Animal models of tuberculosis: Lesson learnt. Indian J Med Res. 2018;147(5):456-63.

19. Kramnik I, Beamer G. Mouse models of human TB pathology: roles in the analysis of necrosis and the development of host-directed therapies. Semin Immunopathol. 2016;38(2):221-37.

20. Snewin VA, Gares MP, Gaora PO, Hasan Z, Brown IN, Young DB. Assessment of immunity to mycobacterial infection with luciferase reporter constructs. Infection and immunity. 1999;67(9):4586-93.

21. Tanghe A, D'Souza S, Rosseels V, Denis O, Ottenhoff TH, Dalemans W, et al. Improved immunogenicity and protective efficacy of a tuberculosis DNA vaccine encoding Ag85 by protein boosting. Infection and immunity. 2001;69(5):3041-7.

22. Cocchi M, Biancolillo A, Marini F. Chapter Ten–Chemometric Methods for Classification and Feature Selection. In: Jaumot J, Bedia C, Tauler R, editors. Comprehensive Analytical Chemistry. 82: Elsevier; 2018. p. 265-99.

23. Romano M, Rindi L, Korf H, Bonanni D, Adnet PY, Jurion F, et al. Immunogenicity and protective efficacy of tuberculosis subunit vaccines expressing PPE44 (Rv2770c). Vaccine. 2008;26(48):6053-63.

24. van Pinxteren LA, Ravn P, Agger EM, Pollock J, Andersen P. Diagnosis of tuberculosis based on the two specific antigens ESAT-6 and CFP10. Clinical and diagnostic laboratory immunology. 2000;7(2):155-60.

25. Commandeur S, Lin MY, van Meijgaarden KE, Friggen AH, Franken KL, Drijfhout JW, et al. Double- and monofunctional CD4(+) and CD8(+) T-cell responses to *Mycobacterium tuberculosis* DosR antigens and peptides in long-term latently infected individuals. European journal of immunology. 2011;41(10):2925-36.

26. Serra-Vidal MM, Latorre I, Franken KL, Diaz J, de Souza-Galvao ML, Casas I, et al. Immunogenicity of 60 novel latency-related antigens of *Mycobacterium tuberculosis*. Frontiers in microbiology. 2014; 5:517.

27. Karbalaei Zadeh Babaki M, Soleimanpour S, Rezaee SA. Antigen 85 complex as a powerful *Mycobacterium tuberculosis* immunogene: Biology, immune-pathogenicity, applications in diagnosis, and vaccine design. Microbial pathogenesis. 2017; 112:20-9.

28. Kaufmann SHE. Vaccination Against Tuberculosis: Revamping BCG by Molecular Genetics Guided by Immunology. Frontiers in immunology. 2020; 11:316.

29. Zaheen A, Bloom BR. Tuberculosis in 2020–New Approaches to a Continuing Global Health Crisis. The New England journal of medicine. 2020;382(14): e26.

30. Lu LL, Smith MT, Yu KKQ, Luedemann C, Suscovich TJ, Grace PS, et al. IFN-gamma-independent immune markers of *Mycobacterium tuberculosis* exposure. Nature medicine. 2019;25(6):977-87.

31. Medina E, North RJ. Resistance ranking of some common inbred mouse strains to *Mycobacterium tuberculosis* and relationship to major histocompatibility complex haplotype and Nramp1 genotype. Immunology. 1998;93(2):270-4.

32. Arko-Mensah J, Rahman MJ, Degano IR, Chuquimia OD, Fotio AL, Garcia I, et al. Resistance to mycobacterial infection: a pattern of early immune responses leads to a better control of pulmonary infection in C57BL/6 compared with BALB/c mice. Vaccine. 2009;27(52):7418-27.

33. Wakeham J, Wang J, Xing Z. Genetically determined disparate innate and adaptive cell-mediated immune responses to pulmonary Mycobacterium bovis BCG infection in C57BL/6 and BALB/c mice. Infection and immunity. 2000;68(12):6946-53.

4

34. Kindler V, Sappino AP, Grau GE, Piguet PF, Vassalli P. The inducing role of tumor necrosis factor in the development of bactericidal granulomas during BCG infection. Cell. 1989;56(5):731-40.

35. Flynn JL, Goldstein MM, Chan J, Triebold KJ, Pfeffer K, Lowenstein CJ, et al. Tumor necrosis factor-alpha is required in the protective immune response against *Mycobacterium tuberculosis* in mice. Immunity. 1995;2(6):561-72.

36. Jayaraman P, Jacques MK, Zhu C, Steblenko KM, Stowell BL, Madi A, et al. TIM3 Mediates T Cell Exhaustion during *Mycobacterium tuberculosis* Infection. PLoS pathogens. 2016;12(3): e1005490.

37. van Dissel JT, Joosten SA, Hoff ST, Soonawala D, Prins C, Hokey DA, et al. A novel liposomal adjuvant system, CAF01, promotes long-lived *Mycobacterium tuberculosis*-specific T-cell responses in human. Vaccine. 2014;32(52):7098-107.

38. Famelis N, Rivera-Calzada A, Degliesposti G, Wingender M, Mietrach N, Skehel JM, et al. Architecture of the mycobacterial type VII secretion system. Nature. 2019;576(7786):321-5.

39. Tufariello JM, Chapman JR, Kerantzas CA, Wong KW, Vilcheze C, Jones CM, et al. Separable roles for *Mycobacterium tuberculosis* ESX-3 effectors in iron acquisition and virulence. Proceedings of the National Academy of Sciences of the United States of America. 2016;113(3):E348-57.

40. Knudsen NP, Norskov-Lauritsen S, Dolganov GM, Schoolnik GK, Lindenstrom T, Andersen P, et al. Tuberculosis vaccine with high predicted population coverage and compatibility with modern diagnostics. Proceedings of the National Academy of Sciences of the United States of America. 2014;111(3):1096-101.

41. Billeskov R, Grandal MV, Poulsen C, Christensen JP, Winther N, Vingsbo-Lundberg C, et al. Difference in TB10.4 T-cell epitope recognition following immunization with recombinant TB10.4, BCG or infection with *Mycobacterium tuberculosis*. European journal of immunology. 2010;40(5):1342-54.

42. Rustad TR, Harrell MI, Liao R, Sherman DR. The enduring hypoxic response of *Mycobacterium tuberculosis*. PloS one. 2008;3(1): e1502.

43. Yu G, Cui Z, Sun X, Peng J, Jiang J, Wu W, et al. Gene expression analysis of two extensively drug-resistant tuberculosis isolates show that two-component response systems enhance drug resistance. Tuberculosis (Edinburgh, Scotland). 2015;95(3):303-14.

44. Gideon HP, Wilkinson KA, Rustad TR, Oni T, Guio H, Sherman DR, et al. Bioinformatic and empirical analysis of novel hypoxia-inducible targets of the human antituberculosis T cell response. Journal of immunology (Baltimore, Md: 1950). 2012;189(12):5867-76.

45. Glickman MS, Cox JS, Jacobs WR, Jr. A novel mycolic acid cyclopropane synthetase is required for cording, persistence, and virulence of *Mycobacterium tuberculosis*. Mol Cell. 2000;5(4):717-27.

46. Hunter RL, Hwang SA, Jagannath C, Actor JK. Cord factor as an invisibility cloak? A hypothesis for asymptomatic TB persistence. Tuberculosis (Edinburgh, Scotland). 2016;101s: S2-s8.

47. Corrales RM, Molle V, Leiba J, Mourey L, de Chastellier C, Kremer L. Phosphorylation of mycobacterial PcaA inhibits mycolic acid cyclopropanation: consequences for intracellular survival and for phagosome maturation block. J Biol Chem. 2012;287(31):26187-99.

48. Deng G, Zhang W, Ji N, Zhai Y, Shi X, Liu X, et al. Identification of Secreted O-Mannosylated Proteins From BCG and Characterization of Immunodominant Antigens BCG_0470 and BCG_0980. Frontiers in microbiology. 2020; 11:407.

49. Tima HG, Al Dulayymi JR, Denis O, Lehebel P, Baols KS, Mohammed MO, et al. Inflammatory Properties and Adjuvant Potential of Synthetic Glycolipids Homologous to Mycolate Esters of the Cell Wall of *Mycobacterium tuberculosis*. J Innate Immun. 2017;9(2):162-80.
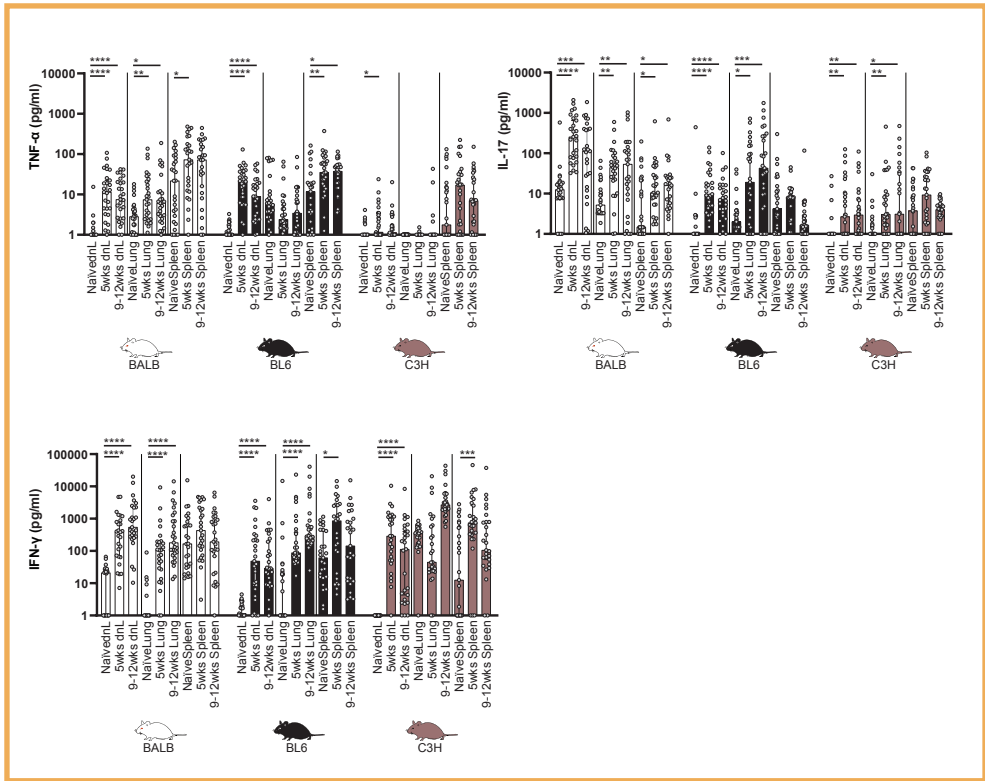
Supplementary Figure 1. Cumulative response against all *Mtb* antigens evaluated in Figure 1. The bar graphs show the TNF-α, IL-17 and IFN-γ production after *Mtb* antigen stimulation of cells from mediastinal lymph nodes (medLN), lungs, and spleens from naïve or *Mtb* infected (five or 9-12 weeks(wks)) C57BL/6 (BL6), BALB/c (BALB) and C3HeB/FeJ (C3H). Dots represent the response against a single antigen, while bars depict the median response against all antigens (*: p<0.05, **: p<0.01, ***: p<0.001, ****: p<0.0001, Kruskal-Wallis test with Dunn's multiple test correction).
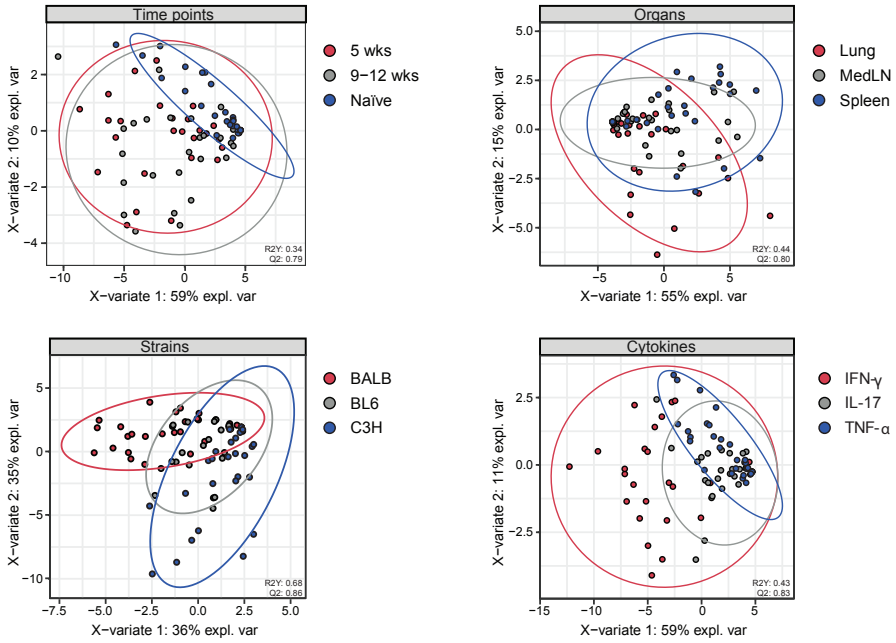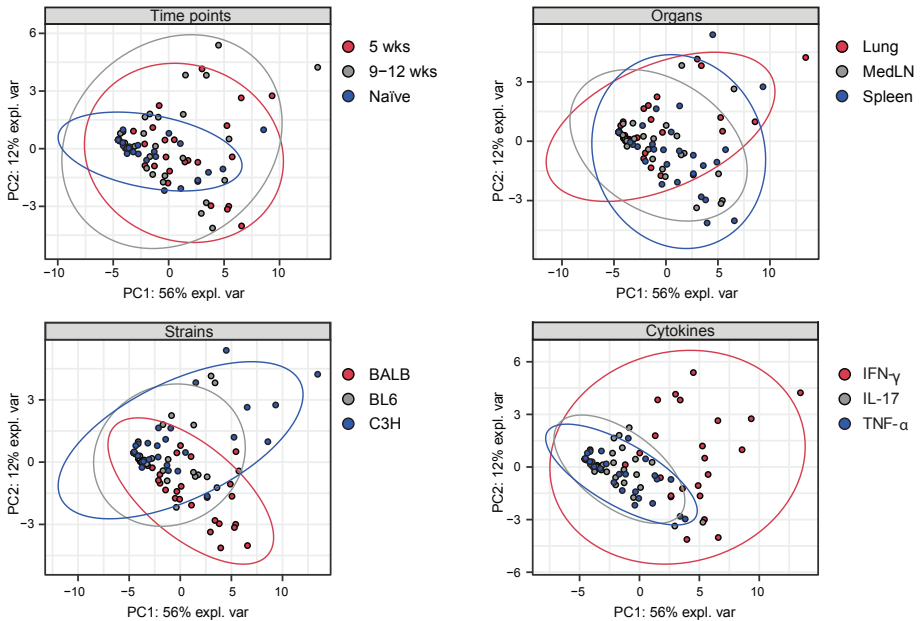
Supplementary Figure 2. PLS-DA and PCA models – related to Figure 1C. (A) PLS-DA and (B) PCA score plots show the separation between antigens on the basis of known classes: (I) time points (i.e., naïve mice vs. mice sacrificed at early or late point after *Mtb* infection) (upper left); (II) mouse strains (i.e., C57BL/6 (BL6), BALB/c (BALB) and C3HeB/FeJ (C3H) mice) (lower left); (III) organs (i.e., lungs, mediastinal lymph nodes or spleens) (upper right); (IV) cytokines (i.e., IFN-γ, TNF-α and IL-17) (lower right). Coloured ovals represent PLS-DA and PCA protein clusters. Dots represent antigens and colour code marks the groups included in each of the models as described in the figure.
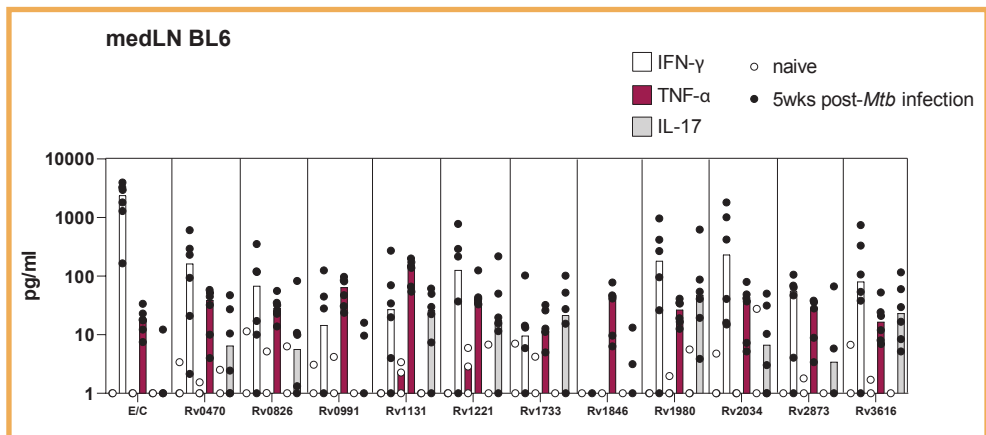
Supplementary Figure 3. Cytokine profiles in response to antigen stimulation in the mediastinal lymph nodes (medLN) of C57BL/6 (BL6) mice – related to Figure 1B. Dot plot graphs depict the TNF-α, IL-17 and IFN-γ production after *Mtb* antigen stimulation of cells from mediastinal lymph nodes (medLN) from C57BL/6 (BL6). White and black solid dots depict the cytokine responses in the naïve and the *Mtb* infected (five weeks (wks) post-infection) groups, respectively. White, purple and grey bars depict the median IFN-γ, TNF-α, and IL-17 concentration, respectively. In this figure are shown antigens that, after FDR correction, induced a significant increase of TNF-α but not IFN-γ or IL-17 in the medLN. ESAT6/CFP10 (E/C) was included for comparison.